Microcellular systems, random walks and wave propagation. *

Massimo Franceschetti Jehoshua Bruck Leonard J. Schulman

California Institute of Technology

Abstract

As the number of users of wireless services increases, the concept of using smaller cell sizes becomes especially attractive because of its potential for capacity increase. Current technology allows to build base stations for small cells in a cost effective way, and telecommunication companies have started exploiting the new microcellular concept in providing coverage to densely populated areas. Prediction of propagation characteristics in this new scenario is essential for accurate link budget calculations in network planning.

In this paper a new, simple model of wave propagation for microcellular systems is applied to predict the path loss of a wireless channel. The model does not rely on the classical theory of electromagnetic wave propagation, but it is entirely based on probability theory. We consider the canonical scenario of a random environment of partially absorbing scatterers and model the trajectory of each photon in the system as a random walk. This model leads to a path loss formula that rather accurately (in comparison to other models and experimental data) describes the smooth transition of power attenuation from an inverse square law with the distance to the transmitter

*This work was partially supported by the Caltech Lee Center for Advanced Networking and by the National Science Foundation under CAREER Grant No. 0049092 (previously 9876172), and by the Charles Lee Powell Foundation.

to an exponential attenuation as this distance is increased. This result can justify empirical formulas that are often used for path loss prediction, characterized by a breakpoint distance at which the exponent of a power law is increased from a value of approximately 2 to a value in the range of 4 to 10.

Theoretical predictions of the model are validated by showing agreement with experimental data collected in the city of Rome, Italy.

Keywords: Wave propagation, path loss, microcellular systems, random media.

1 Introduction and Background

In the last few years the concept of microcellular systems used for wireless personal communication has attracted much attention [11]. A microcell is a region served by a radio base station, smaller than traditional macrocells by one or two orders of magnitude. This reduction in size is usually obtained by transmitting at low power (typically below 10W), and by using low antennas (typically below 10m), and has the advantage of increasing the overall capacity of the system.

Prediction of propagation characteristics is essential for link budget calculations in wireless network planning, therefore models, algorithms, and mathematical tools for prediction of the electromagnetic signal characteristics in the new microcellular scenario are of critical importance.

Propagation in microcells has been investigated in both line of sight (LOS) and non line of sight (NLOS) conditions. In both cases, in almost all work, the propagation loss is modelled using an inverse power law in the distance to the transmitter. This inverse power law model goes back to the empirical formula given by Hata [13], following previous work of Okumura et al. [17], based on extensive experimental measurements made in the nineteen-sixties in Japan. When adapting the Okumura-Hata model to microcellular systems, there is experimental evidence of a power law exponent that increases as a function of the distance between the transmitter and the receiver. To accommodate to this variation, telecommunication companies have gained some familiarity in using path loss models characterized by a breakpoint distance at which the exponent of the inverse power law is changed. The existence of such a breakpoint can be theoretically justified, in LOS conditions, using a simple two-ray propagation model consisting of the direct and ground reflected ray. This model predicts the existence of a breakpoint distance r_b at which the characteristic of power loss with distance r from the transmitter is changed from the mode r^{-2} (for $r < r_b$) to the mode r^{-4} (for $r > r_b$), and has been used in [21] to predict LOS power attenuation in microcellular systems. The model can also be refined considering the two additional rays reflected by

the buildings along the street, but this extension does not change the predicted transition to the r^{-4} mode [2] [18]. Hence, this simple ray model cannot explain the experimentally observed power loss modes of r^{-q}, with q in the range 4 to 10 beyond the breakpoint [3] [4] [5] [7] [10]. Recently, a new multislit waveguide model for describing wave propagation along straight streets with randomly distributed walls of buildings and gaps between them, has been proposed in [3] [4] [5]. This model predicts a smooth transition from an r^{-2} mode to an exponential attenuation mode that can explain the empirical high order power law of r^{-q}, $q > 4$, obtained in most experiments.

In NLOS conditions empirical path loss formulas of the type r^{-q} have also been used and, by using low transmitting antennas, values of q considerably larger than 4 after a breakpoint have been found [6]. In this case the propagation mechanism must be based on multiple scattering and diffraction effects that allow coverage of NLOS locations. For example, in urban microcellular systems, lamp posts, street signs, trees and vegetation, pedestrians, cars, irregularly sited and textured building walls (common in older European constructions), can scatter energy in many directions, allowing reception of signal in shaded areas. These effects are typically difficult to predict, and additional efforts have been made to develop approximate models that can justify the experimental findings. Xia et al. [15] [20] proposed a model based on multiple forward diffraction over a row of parallel, equispaced buildings of the same height. Their model, however, can only predict values of the path loss exponent q less than 4.5. Recently, Franceschetti G. et al. [8] [16] proposed a new analytic model based on random walks, rather than wave interference effects. They model a city as a random medium of lossless scatterers and consider a random walk formulation of the problem of optical ray penetration inside the medium. Their study, however, not considering signal attenuation inside the medium, nor considering locating the transmitter inside the medium, does not lead to a path loss formula that can be experimentally validated.

In this paper we present a new probabilistic model of propagation in cluttered environments that leads to a path loss formula that rather accurately (in comparison to other models and to the experimental data) describes the smooth transition of power attenuation

from the free space mode r^{-2} to an exponential attenuation, and that is, in the medium range, close to the empirical formulas that use high order power laws, after a breakpoint, to fit experimental data. The model is solved analytically and its theoretical predictions are validated by showing agreement with experimental data collected in the city of Rome, Italy.

We refer to the canonical scenario described in Fig. 1. A monochromatic isotropic wave radiated by a transmitter reaches the intended receiver undergoing multiple scattering from different obstacles placed in the environment. The scattering mechanism is lossy: at each reflection the wave undergoes a prescribed attenuation. This physical picture is modelled in probabilistic terms. The wave is composed of emitted photons that move following a piecewise linear random walk inside the medium. We assume that each time a photon hits an obstacle, it has a probability γ of being absorbed, and a probability $(1-\gamma)$ of being scattered in a random direction. We are interested in computing both the power density and the power flux at distance r from the transmitter. The former equals the number of photons entering an infinitesimal sphere of radius Δr placed at distance r, normalized to the sphere surface; the latter is defined as the number of photons leaving a sphere centered at the transmitter and of radius r, normalized to the sphere surface. Both quantities are related to the probability density function (*pdf*) of a photon to be absorbed at a distance r from the source. We derive exact (in 1D) and approximate (in 2D and 3D) analytical formulas for this power density and power flux, as functions of the absorption coefficient γ and of the average step length $1/\eta$ of the random walk (which is essentially a measure of the density of obstacles in the environment). Our main theoretical result is in proving a propagation loss that follows (in 3D) an inverse square law with the distance to the transmitter, with a smooth transition to an exponential mode as the distance between transmitter and receiver increases (see Fig. 2). An advantage of the model is that it does not necessarily rely on experimental data to tune the parameters γ and η using regression analysis (as is common with empirical formulas): in principle, these parameters can be chosen by estimating directly the amount of clutter in the environment and the absorption coefficient of the scatterers, which can be less expensive than performing experiments. Indeed, when we compare our

model with experimental data, we find values of the parameters that correspond to having on average one obstacle every ten meters, with an absorption coefficient of $12\% \sim 17\%$, which is reasonable for the urban area considered.

We understand that our probabilistic modelling of the physical picture in Fig. 1 is an oversimplified version of the real propagation problem. Our random walk formulation essentially assumes the obstacles to be small, thus re-radiating as point sources. Popular numerical solvers, based on ray tracing techniques, assume, on the contrary, that the obstacles are large and planar, thus re-radiating according to the laws of geometrical optics. However, there is numerical and experimental evidence [19] that these solvers underestimate the real attenuation, when used to predict the path loss in microcells. In [19] it is shown that better matching with experimental data is obtained by decomposing the large obstacles into smaller, more uniformly scattering patches.

Finally, we point out the existence of a huge literature on wave propagation in random media, that is usually not accounted for in more recent cellular communication works. A good, comprehensive reference book on the subject is the one by Ishimaru [14]. Where possible, we highlight similarities between formulas obtained in our model and corresponding formulas derived from electromagnetics as described in [14]. In particular, in Section 6 we show how our model allows an interpretation of the results of the transport theory of propagation in the light of the recurrence properties of random walks. We believe that it is quite intriguing to find such relationships between models that are based on such different premises.

The rest of the paper is divided into two parts. In part I we present our theoretical model of propagation, discuss exact and approximate analytical solutions in 1,2, and 3 dimensions, and we compare results with the classical theory. In part II we validate the results of the model with experimental measurements and introduce a simplified path loss formula that can be used for quick, practical prediction purposes.

Part I: The wandering photon

2 Summary

We model the trajectory of each photon radiating from an isotropic narrowband source as a piecewise linear random walk with absorbing probabilities (see Fig. 1). The average step length of the random walk is $1/\eta$, and we assume that each time the photon is about to turn in a random direction, it can be absorbed, with probability γ, by the reflecting obstacle and hence stop its random walk. Our procedure consists in finding an expression for the *pdf* of the site where the random walk stops and then to obtain an expression for the radiated power flux and power density at a given distance from the transmitter. Our model is solved exactly in one dimension, and with some approximation in two and three dimensions. In all cases, the approximate formulas are compared with a numerical estimate of the corresponding exact formulas, demonstrating the validity of the approximation within a small error. Finally, a comparison with the classical theory is given.

3 One dimension

We start by looking at the one dimensional case. In one dimension the trajectory of a photon occurs along a single straight line. We imagine each photon to behave as a sleepy drunk person walking on the line. The drunk proceeds at a constant pace but at random, Poisson distributed intervals, he trips, at which point with probability γ he falls asleep, and with probability $(1-\gamma)/2$ he continues in each direction. Accordingly, let x be the coordinate of the line, and H be the *pdf*:

$$H(x) = \eta e^{-\eta x}, \quad (x \geq 0)$$

and let $\overline{H}(x)$ be the "flipped" density:

$$\overline{H}(x) = \eta e^{\eta x}, \quad (x \leq 0).$$

The overall *pdf* of finding an obstacle at x, in the first step of the random walk, is given by:

$$Q(x) = \frac{H + \overline{H}}{2} = \frac{\eta}{2} e^{-\eta|x|}.$$

We are now interested in the *pdf* $G(x)$ of the site where the drunk falls asleep. With $*$ indicating convolution, this density can be found by solving the equation:

$$G(x) = \gamma Q(x) + (1-\gamma) Q * G(x). \tag{1}$$

Use of Eq. (1) can be justified as follows. Let us iteratively substitute the expression for $G(x)$ in the convolution integral. We have $G(x) = G_0(x) + G_1(x) + G_2(x) + \ldots$, with $G_0(x) = \gamma Q(x)$, $G_1(x) = (1-\gamma)Q(x) * G_0(x)$, $G_2(x) = (1-\gamma)Q(x) * (1-\gamma)Q(x) * G_0(x), \ldots$ $G_0(x)$ describes the event that the drunk falls asleep at the first step of the random walk, hitting a single obstacle. $G_1(x)$ describes the event that the drunk falls asleep at the second step, hitting two obstacles and so on. Since all these events are disjoint, we sum all the G_i's to obtain the overall *pdf* $G(x)$ of the site where the drunk falls asleep.

The convolution in Eq. (1) suggests examining the Fourier transforms (characteristic functions in the terminology of probability theory) of the probability densities.

Let $g(\omega), h(\omega), \overline{h}(\omega)$ be the Fourier transforms (FT) of $G(x), H(x), \overline{H}(x)$ respectively. In particular:

$$h(\omega) = \eta \int_0^\infty e^{-\eta x} e^{-i\omega x} dx = \frac{\eta}{\eta + i\omega} \quad (\eta > 0),$$

$$\overline{h}(\omega) = h^*(\omega) \quad (\eta > 0).$$

$$q(\omega) = \frac{h(\omega) + \overline{h}(\omega)}{2} = \frac{\eta^2}{\eta^2 + \omega^2}$$

Noting that $H * \overline{H} = \frac{H + \overline{H}}{2} = Q$, we can write the analogue of Eq (1) in the Fourier domain as:

$$g(\omega) = \gamma h(\omega) h^*(\omega) + (1-\gamma) h(\omega) h^*(\omega) g(\omega). \tag{2}$$

By solving for $g(\omega)$ we have:

$$g(\omega) = \frac{\gamma \eta^2}{\omega^2 + \gamma \eta^2}$$

and by inverse FT we find:

$$G(x) = \frac{\sqrt{\gamma}\eta}{2} e^{-\eta\sqrt{\gamma}|x|}. \tag{3}$$

Discussion of Eq (3) is now in order. Note that there is only one independent parameter, $\eta\sqrt{\gamma}$, for this family of distributions; the absorption probability γ and the obstacle density η can be traded off against each other without affecting the distribution. As a check on this equation note that, for $\gamma = 1$ (perfectly opaque obstacles), the drunk falls asleep at the first step, and we have $G(x) = Q(x)$. Moreover, as the probability γ of the drunk falling asleep at each given obstacle tends to zero, the density spreads more widely over the real line ($\eta\sqrt{\gamma} \to 0$).

Quantitatively, Eq (3) provides an elegant prediction: at any fixed level of clutter in the environment, the effective radius of the signal scales as the square root of $1/\gamma$, the expected number of steps taken by the random walk. This phenomenon is closely related to the square-root-of-time scaling of the distance travelled by a symmetric random walk; however, the actual distributions in the two processes are quite different, being in this case a two-sided exponential rather than a normal distribution.

We can now obtain the average transmitted power flux at a distance $x_0 > 0$ from the origin, when radiating a narrowband signal of unitary amplitude:

$$F(x_0) = \int_{x_0}^{\infty} G(x)dx = \frac{e^{-\eta\sqrt{\gamma}x_0}}{2}.$$

Note that when there are no obstacles ($\eta = 0$), or when there is no absorbtion ($\gamma = 0$), $F(x_0) = 1/2$ as the power splits evenly along the two directions of the lossless, obstacle free line.

4 Two dimensions

We now turn our attention to the two dimensional case. Solutions, in this case, will be described in terms of Bessel functions. The immediate generalization of Eq. (2) to two

dimensions is:

$$G(r) = \gamma Q(r) + (1-\gamma) Q * G(r), \tag{4}$$

where $G(r)$ is the probability of the drunk falling asleep at a given radial distance r from the origin, and the probability density $Q(r)$ of the drunk finding the first obstacle at a radial distance r from the origin is given by:

$$Q(r) = \frac{\eta e^{-\eta r}}{2\pi r}.$$

For subsequent analysis, the FT of $Q(r)$ is needed:

$$q(u,v) = \int_{-\infty}^{+\infty} \int_{-\infty}^{+\infty} \frac{\eta e^{-\eta\sqrt{x^2+y^2}}}{2\pi\sqrt{x^2+y^2}} e^{-iux} e^{-ivy} dx dy.$$

By letting $x = r\cos\phi$, $y = r\sin\phi$, $u = \omega\cos\psi$, $v = \omega\sin\psi$, we have, for ω = distance from the origin:

$$q(\omega) = \frac{\eta}{2\pi} \int_0^{\infty} e^{-\eta r} dr \int_0^{2\pi} e^{-i\omega r\cos(\phi-\psi)} d\phi =$$

$$= \frac{\eta}{2\pi} \int_0^{\infty} e^{-\eta r} dr \int_0^{2\pi} \sum_{k=-\infty}^{+\infty} (-i)^k J_k(\omega r) e^{-ik(\phi-\psi)} d\phi =$$

$$= \eta \int_0^{\infty} e^{-\eta r} J_0(\omega r) dr,$$

where we have used the Bessel expansion 8.511.4 in ref. [9]. Then, by exploiting identity 6.611.1 of ref. [9], we obtain:

$$q(\omega) = \frac{\eta}{\sqrt{\eta^2+\omega^2}}.$$

Substituting $q(\omega)$ into the FT of eq.(4), and solving for $g(\omega)$, we obtain:

$$g(\omega) = \frac{\gamma\eta}{\sqrt{\eta^2+\omega^2} - (1-\gamma)\eta},$$

and by inverse FT we obtain:

$$G(r) = \frac{\gamma\eta}{(2\pi)^2} \int_0^{\infty} \frac{\omega}{\sqrt{\eta^2+\omega^2} - (1-\gamma)\eta} d\omega \int_0^{2\pi} e^{i\omega r\cos(\psi-\phi)} d\psi =$$

$$= \frac{\gamma\eta}{(2\pi)^2} \int_0^{\infty} \frac{\omega}{\sqrt{\eta^2+\omega^2} - (1-\gamma)\eta} d\omega \int_0^{2\pi} \sum_{k=-\infty}^{+\infty} i^k J_k(\omega r) e^{ik(\psi-\phi)} d\psi =$$

$$= \frac{\gamma\eta}{2\pi}\int_0^\infty \frac{\omega J_0(\omega r)}{\sqrt{\omega^2+\eta^2}-(1-\gamma)\eta}d\omega. \tag{5}$$

Note that, for $\gamma = 1$ (perfectly opaque obstacles), the drunk falls asleep at the first step, and the integral reduces to:

$$G(r) = \frac{\eta}{2\pi}\int_0^\infty \frac{\omega J_0(\omega r)}{\sqrt{\omega^2+\eta^2}}d\omega = \frac{\eta e^{-\eta r}}{2\pi r} = Q(r),$$

as expected, see identity 6.554.1 in ref. [9].

In the general case of $\gamma \neq 1$ the integral in (5) is non-trivial to compute. In the following, we show an exact solution, expressed in terms of an infinite series of polynomials, and a corresponding approximate solution in closed form.

4.1 Exact Solution

In this section we show the exact derivation of $G(r)$, written as a series of Bessel polynomials. Let $\alpha = \eta(1-\gamma)$. We rewrite Eq. (5) as follows:

$$G(r) = \frac{\gamma\eta}{2\pi}\int_0^\infty \frac{\omega J_0(\omega r)}{\sqrt{\omega^2+\eta^2}-\alpha}d\omega =$$

$$= \frac{\gamma\eta}{2\pi}\int_0^\infty \frac{\omega J_0(\omega r)}{\omega^2+\eta^2-\alpha^2}\left(\sqrt{\omega^2+\eta^2}+\alpha\right)d\omega =$$

$$= \frac{\gamma\eta}{2\pi}\left[\alpha\int_0^\infty \frac{\omega J_0(\omega r)}{\omega^2+\eta^2-\alpha^2}d\omega + \int_0^\infty \frac{\omega J_0(\omega r)\sqrt{\omega^2+\eta^2}}{\omega^2+\eta^2-\alpha^2}d\omega\right] =$$

$$= \frac{\gamma\eta}{2\pi}\left(\widehat{\mathcal{I}}_1+\widehat{\mathcal{I}}_2\right) = \frac{\gamma\eta}{2\pi}\left[\alpha K_0(\sqrt{\eta^2-\alpha^2}r)+\widehat{\mathcal{I}}_2\right],$$

having used identity 6.532.4, in ref. [9], to calculate integral $\widehat{\mathcal{I}}_1$. We can then write integral $\widehat{\mathcal{I}}_2$ as a series of integrals,

$$\widehat{\mathcal{I}}_2 = \int_0^\infty \frac{\omega J_0(\omega r)}{\sqrt{\omega^2+\eta^2}\left(1-\frac{\alpha^2}{\omega^2+\eta^2}\right)}d\omega =$$

$$= \int_0^\infty \frac{\omega J_0(\omega r)}{\sqrt{\omega^2+\eta^2}}\sum_{n=0}^\infty \frac{\alpha^{2n}}{(\omega^2+\eta^2)^n}d\omega = \sum_{n=0}^\infty \alpha^{2n}\int_0^\infty \frac{\omega J_0(\omega r)}{(\omega^2+\eta^2)^{n+1/2}}d\omega = \sum_{n=0}^\infty \mathcal{I}_n.$$

We have the following recurrence relation:

$$\begin{cases} \mathcal{I}_0 = & \displaystyle\int_0^\infty \frac{\omega J_0(\omega r)}{\sqrt{\omega^2+\eta^2}} d\omega = \frac{e^{-\eta r}}{r} \\ \\ \mathcal{I}_{n+1} = & \displaystyle\frac{-\alpha^2}{(2n+1)} \frac{1}{\eta} \frac{\partial}{\partial \eta} \mathcal{I}_n. \end{cases} \tag{6}$$

We recall that Bessel polynomials [12] are defined as:

$$\theta_n(z) = \sum_{j=0}^{n} a_j z^{n-j},$$

where all coefficients are integers given by

$$a_j = \frac{(n+j)!}{2^j\ (n-j)!\ j!}.$$

From the recurrence (6) and the definition of θ_n, it follows that:

$$\widehat{\mathcal{I}}_2 = \sum_{n=0}^{\infty} \mathcal{I}_n = \frac{e^{-\eta r}}{r} \left[1 + \eta r \sum_{n=0}^{\infty} c_n \theta_n(\eta r) \right], \tag{7}$$

where

$$c_n = \frac{(1-\gamma)^{2(n+1)}}{(2n+1)!!},$$

which gives the following exact formula for $G(r)$,

$$G(r) = \frac{\gamma \eta^2}{2\pi} \left[\frac{e^{-\eta r}}{\eta r} \left(1 + \eta r \sum_{n=0}^{\infty} c_n \theta_n(\eta r) \right) + (1-\gamma) K_0(\sqrt{\eta^2 - \alpha^2} r) \right]. \tag{8}$$

4.2 Approximate Solution

In order to obtain an approximate solution in closed form for the integral in Eq. (5), we look at the Taylor expansion, with respect to η, of the function:

$$\frac{e^{-(\eta - \frac{\alpha^2}{\eta})r}}{r} = \sum_{n=0}^{\infty} \frac{1}{n!} \left(-\frac{\alpha^2}{\eta} \right)^n \frac{\partial^n}{(\partial \eta)^n} \left(\frac{e^{-\eta r}}{r} \right), \tag{9}$$

and note that the first two terms of this expansion are the same as the first two terms of eq. (7). Therefore, neglecting higher order terms in Eqs. (7) and (9), we can write:

$$\widehat{\mathcal{I}}_2 \approx \frac{e^{-(\eta-\frac{\alpha^2}{\eta})r}}{r},$$

and obtain the desired approximation:

$$G(r) \approx \frac{\gamma\eta}{2\pi}\left[\frac{e^{-\frac{\eta^2-\alpha^2}{\eta}r}}{r} + \alpha K_0(\sqrt{\eta^2-\alpha^2}r)\right]. \tag{10}$$

We now discuss the validity of the approximation in Eq. (10). Letting $\eta r = R$, we have:

$$G(R) = \frac{\gamma\eta^2}{2\pi}\left[\frac{e^{-R}}{R}\left(1 + R\sum_{n=0}^{\infty} c_n\theta_n(R)\right) + (1-\gamma)K_0(\sqrt{1-(1-\gamma)^2}R)\right] =$$

$$\approx Appr(R) = \frac{\gamma\eta^2}{2\pi}\left[\frac{e^{-R}}{R}\ e^{(1-\gamma)^2 R} + (1-\gamma)K_0(\sqrt{1-(1-\gamma)^2}R)\right].$$

Note that it would be misleading to refer to the relative error, because both $G(R)$ and $Appr(R)$ tend to zero, as $R \to \infty$. Accordingly, we evaluate the absolute error. Letting $Err = G - Appr$, we depict in Fig. 3 a plot of the function:

$$\left(\frac{2\pi Err}{\eta^2}\right)^2 = \left\{\gamma\frac{e^{-R}}{R}\left[1 + R\sum_{n=0}^{\infty} c_n\theta_n(R) - e^{(1-\gamma)^2 R}\right]\right\}^2;$$

numerical estimation suggests that the error is bounded by:

$$|Err| < \frac{\sqrt{0.0027}}{2\pi}\eta^2.$$

Note that, in spite of being an approximation, Eq. (10) integrates to one as expected by a probability density:

$$\int_0^{2\pi} d\phi \int_0^{\infty} r\frac{\gamma\eta}{2\pi}\left[\frac{e^{-\frac{\eta^2-\alpha^2}{\eta}r}}{r} + \alpha K_0(\sqrt{\eta^2-\alpha^2}r)\right] dr =$$

$$= \gamma\eta\left(\frac{\eta}{\eta^2-\alpha^2} + \frac{\alpha}{\eta^2-\alpha^2}\right) = \frac{\gamma\eta}{\eta-\alpha} = 1.$$

Moreover, when $\gamma = 1$, $Err = 0$, and $G(r) = Q(r)$ as expected.

Finally, exploiting the approximation in Eq. (10), we can calculate the approximate average power flux at a distance $r_0 > 0$ from the origin, when radiating a narrowband signal of unitary amplitude:

$$F(r_0) = \frac{1}{2\pi r_0} \int_0^{2\pi} d\phi \int_{r_0}^{\infty} rG(r)dr =$$

$$= \frac{1}{2\pi r_0} \left[\frac{1}{2-\gamma} e^{-\frac{\eta^2-\alpha^2}{\eta} r_0} + \frac{\sqrt{\gamma}\eta(1-\gamma)}{\sqrt{2-\gamma}} r_0 K_1(\sqrt{\eta^2-\alpha^2} r_0) \right], \tag{11}$$

see identity 5.52.1 in ref. [9].

It is interesting to check two limiting cases. When there are no obstacles ($\eta = 0$) we have:

$$F(r_0) = \frac{1}{2\pi r_0} \left[\frac{1}{2-\gamma} + \frac{\sqrt{\gamma}\eta(1-\gamma)}{\sqrt{2-\gamma}} r_0 K_1(z \to 0) \right] =$$

$$= \frac{1}{2\pi r_0} \left(\frac{1}{2-\gamma} + \frac{1-\gamma}{2-\gamma} \right) = \frac{1}{2\pi r_0},$$

having used the series expansion 8.446, of ref. [9], for $K_1(z)$. Similarly, when we have no absorbtion ($\gamma = 0$), we have:

$$F(r_0) = \frac{1}{2\pi r_0} \left(\frac{1}{2} + \frac{1}{2} \right) = \frac{1}{2\pi r_0},$$

as in the case of propagation of a cylindrical wave over a free plane.

5 Three dimensions

In the three dimensional case $Q(r)$ becomes:

$$Q(r) = \eta \frac{e^{-\eta r}}{4\pi r^2},$$

and its FT, $q(\omega)$, is given by

$$q(\omega) = \int_0^{2\pi} d\phi \int_0^{\pi} \sin\theta d\theta \int_0^{\infty} r^2 e^{-i\omega\cos\theta r} Q(r)dr =$$

$$= \frac{\eta}{2} \int_0^{\pi} \sin\theta d\theta \int_0^{\infty} e^{-(\eta + i\omega\cos\theta)r} dr = \frac{\eta}{2} \int_0^{\pi} \frac{\sin\theta}{\eta + i\omega\cos\theta} d\theta =$$

$$= \frac{\eta}{\omega} \arctan \frac{\omega}{\eta}.$$

By substituting $q(\omega)$ into the Fourier tranform of the equation:

$$G(r) = \gamma Q(r) + (1-\gamma) Q * G(r) \tag{12}$$

and solving for $g(\omega)$ we obtain:

$$g(\omega) = \frac{\gamma \frac{\eta}{\omega} \arctan \frac{\omega}{\eta}}{1 - (1-\gamma)\frac{\eta}{\omega} \arctan \frac{\omega}{\eta}}; \tag{13}$$

by inverse FT we have,

$$G(r) = \frac{1}{(2\pi)^3} \int_0^{2\pi} d\phi \int_0^{\pi} \sin\theta d\theta \int_0^{\infty} \omega^2 g(\omega) e^{i\omega r \cos\theta} d\omega =$$

$$= \frac{1}{(2\pi)^2} \int_0^{\infty} \omega^2 g(\omega) d\omega \int_0^{\pi} \sin\theta \; e^{i\omega r \cos\theta} d\theta = \frac{2}{(2\pi)^2} \int_0^{\infty} \omega^2 g(\omega) \mathrm{sinc}(\omega r) d\omega, \tag{14}$$

where we have defined $\mathrm{sinc}\, x = (\sin x)/x$.

Before proceeding further we note that the integrand in Eq. (14) oscillates as $\sin(\omega r)$, for $\omega \to \infty$. We ignore this, for the time being, and we regularize later the integrand behavior for large values of ω, making it well defined.

We now use the following approximation (see ref. [9], 1.644.1),

$$\arctan \frac{\omega}{\eta} \approx \frac{\omega/\eta}{\sqrt{1 + \left(\frac{\omega}{\eta}\right)^2}},$$

that is accurate for small values of the argument. For large values of the argument ($\omega >> \eta$), first we note that this approximation does not change the observed oscillatory behavior of the integrand. Moreover, we note that for $\omega >> \eta$ the bounded error of the approximation does not affect the evaluation of the integral, because, for large values of ω and after regularization, the integrand provides a negligible contribution to the integral.

Substituting Eq (13) into Eq. (14) we obtain

$$G(r) \approx \frac{2}{(2\pi)^2} \int_0^{\infty} \omega^2 \frac{\gamma\eta}{\sqrt{\eta^2 + \omega^2} - (1-\gamma)\eta} \mathrm{sinc}(\omega r) d\omega =$$

$$= \frac{\gamma\eta}{(2\pi)^2}\left[(1-\gamma)\eta\int_{-\infty}^{+\infty}\frac{\omega^2\mathrm{sinc}(\omega r)}{\omega^2+\eta^2-(1-\gamma)^2\eta^2}d\omega + \int_{-\infty}^{+\infty}\frac{\omega^2\sqrt{\eta^2+\omega^2}\mathrm{sinc}(\omega r)}{\omega^2+\eta^2-(1-\gamma)^2\eta^2}d\omega\right] =$$

$$= \frac{\gamma\eta}{(2\pi)^2}\left(\widehat{\mathcal{I}}_1+\widehat{\mathcal{I}}_2\right) = \frac{\gamma\eta}{(2\pi)^2}\left[(1-\gamma)\eta\frac{\pi}{r}\,e^{-\sqrt{1-(1-\gamma)^2}\eta r}+\widehat{\mathcal{I}}_2\right], \tag{15}$$

having used identities 3.721.1, 3.725.1 in ref. [9] to calculate integral $\widehat{\mathcal{I}}_1$. Note that the oscillatory behavior of the integrand is limited to $\widehat{\mathcal{I}}_2$. In the following we first make $\widehat{\mathcal{I}}_2$ well defined, by integrating its integrand with respect to r, and then, by following a similar procedure as the one employed in Section 4, we calculate $\widehat{\mathcal{I}}_2$ by writing it as a series of integrals and exploiting a recurrence relation. Letting $\alpha = \eta(1-\gamma)$, we have:

$$\widehat{\mathcal{I}}_2 = \int_{-\infty}^{+\infty}\frac{\omega\sqrt{\eta^2+\omega^2}}{\omega^2+\eta^2-\alpha^2}\;\frac{e^{i\omega r}-e^{-i\omega r}}{2ir}\,d\omega =$$

$$= \frac{1}{ir}\int_{-\infty}^{+\infty}\frac{\omega\sqrt{\eta^2+\omega^2}}{\omega^2+\eta^2-\alpha^2}\,e^{i\omega r}d\omega = -\frac{1}{r}\frac{\partial}{\partial r}\int_{-\infty}^{+\infty}\frac{\sqrt{\eta^2+\omega^2}}{\omega^2+\eta^2-\alpha^2}\,e^{j\omega r}d\omega =$$

$$= -\frac{2}{r}\frac{\partial}{\partial r}\int_0^{+\infty}\frac{\cos\omega r}{\sqrt{\omega^2+\eta^2}}\sum_{n=0}^{\infty}\left(\frac{\alpha^2}{\omega^2+\eta^2}\right)^n d\omega =$$

$$= -\frac{2}{r}\frac{\partial}{\partial r}\sum_{n=0}^{\infty}\int_0^{+\infty}\frac{\alpha^{2n}\cos\omega r}{(\omega^2+\eta^2)^{n+1/2}}d\omega = -\frac{2}{r}\frac{\partial}{\partial r}\sum_{n=0}^{\infty}\mathcal{I}_n,$$

where we have defined $\mathcal{I}_n = \int_0^{+\infty}\frac{\alpha^{2n}\cos\omega r}{(\omega^2+\eta^2)^{n+1/2}}d\omega$. Note that the integration with respect to r performed above introduces a decay of the integrand for large values of ω, thus rendering $\widehat{\mathcal{I}}_2$ well defined. We now have a recurrence relation similar to equation (6):

$$\begin{cases}\mathcal{I}_0 = \displaystyle\int_0^{\infty}\frac{\cos\omega r}{\sqrt{\omega^2+\eta^2}}d\omega = K_0(\eta r)\\[2ex] \mathcal{I}_{n+1} = \dfrac{-\alpha^2}{(2n+1)}\dfrac{1}{\eta}\dfrac{\partial}{\partial\eta}\mathcal{I}_n;\end{cases} \tag{16}$$

where the expression for $\mathcal{I}_0$ has been obtained by exploiting identity 3.754.2 in ref. [9]. Following the same procedure as in Section 4.2, we now look at the first two terms of recurrence (16) and note that these correspond to the first two terms of the Taylor expansion, with respect to η, of the function:

$$K_0\left[\left(\eta-\frac{\alpha^2}{\eta}\right)r\right].$$

Hence, neglecting the higher order terms of the expansion, we have the following:

$$\widehat{\mathcal{I}_2} = -\frac{2}{r}\frac{\partial}{\partial r}\sum_{n=0}^{\infty}\mathcal{I}_n \approx -\frac{2}{r}\frac{\partial}{\partial r}K_0\left[\left(\eta - \frac{\alpha^2}{\eta}\right)r\right] =$$

$$= 2\eta\frac{1-(1-\gamma)^2}{r}K_1[(1-(1-\gamma)^2)\eta r]. \tag{17}$$

Substituting Eq. (17) into Eq. (15) we finally obtain the desired approximation:

$$G(r) \approx \frac{\gamma\eta}{4\pi r^2}\left\{\eta r(1-\gamma)e^{-\sqrt{1-(1-\gamma)^2}\eta r} + \frac{2}{\pi}[1-(1-\gamma)^2]\eta r\ K_1[(1-(1-\gamma)^2)\eta r]\right\}. \tag{18}$$

As a check, note that, in spite of being an approximation, the expression in Eq. (18) integrates to one, and so it is a probability density:

$$\int\int\int G(r)d\underline{\mathbf{v}} = \int_0^{2\pi}d\phi\int_0^{\pi}\sin\theta d\theta\int_0^{\infty}r^2G(r)dr =$$

$$= \gamma\eta^2\left\{(1-\gamma)\int_0^{\infty}re^{-\sqrt{1-(1-\gamma)^2}\eta r}dr + \frac{2}{\pi}[1-(1-\gamma^2)]\int_0^{\infty}rK_1[(1-(1-\gamma)^2)\eta r]\right\} =$$

$$= \gamma\eta^2\left\{\frac{1-\gamma}{[1-(1-\gamma)^2]\eta^2} + \frac{2}{\pi}\frac{1-(1-\gamma)^2}{[1-(1-\gamma)^2]^2\eta^2}\ \Gamma(3/2)\ \Gamma(1/2)\right\} =$$

$$= \frac{\gamma(2-\gamma)}{1-(1-\gamma)^2} = 1,$$

having used identity 6.561.16 in ref. [9].

Finally, exploiting the approximation in Eq. (18), we can calculate the approximate average power flux at a distance $r_0 > 0$ from the origin, when radiating a narrowband signal of unitary amplitude:

$$F(r_0) = \frac{1}{4\pi r_0^2}\int_0^{2\pi}d\phi\int_0^{\pi}\sin\theta d\theta\int_{r_0}^{\infty}r^2G(r)dr =$$

$$= \frac{\gamma\eta^2(1-\gamma)}{4\pi r_0^2}\int_{r_0}^{\infty}re^{-\sqrt{1-(1-\gamma)^2}\eta r}dr - \frac{1}{4\pi r_0^2}\ \frac{2\gamma\eta}{\pi}\int_{r_0}^{\infty}r\frac{\partial}{\partial r}K_0[(1-(1-\gamma)^2)\eta r]dr =$$

$$= \frac{1}{4\pi r_0^2}\ \frac{\gamma(1-\gamma)}{1-(1-\gamma)^2}\left(\sqrt{1-(1-\gamma)^2}\eta r_0 + 1\right)e^{-\sqrt{1-(1-\gamma)^2}\eta r_0} + \frac{\gamma\eta}{2\pi^2 r_0^2}\left\{r_0K_0[(1-(1-\gamma)^2)\eta r_0] + \right.$$

$$\left. + \int_{r_0}^{\infty}K_0[(1-(1-\gamma)^2)\eta r]dr\right\}. \tag{19}$$

Letting $[1-(1-\gamma)^2]\eta = \beta$, we use the asymptotic approximation 8.451.6 for $K_0(\cdot)$ in ref. [9] to calculate the last integral in Eq. (19):

$$\int_{r_0}^{\infty} K_0(\beta r)dr = \frac{1}{\beta}\int_{\beta r_0}^{\infty} K_0(x)dx \approx \frac{1}{\beta}\sqrt{\frac{\pi}{2}}\int_{\beta r_0}^{\infty}\frac{1}{\sqrt{x}}\,e^{-x}dx =$$

$$= \frac{1}{\beta}\,\sqrt{2\pi}\int_{\sqrt{\beta r_0}}^{\infty} e^{-u^2}du = \frac{\pi}{\sqrt{2}\beta}\,\mathrm{Erfc}(\sqrt{\beta r_0}) \tag{20}$$

having defined $u=\sqrt{x}$, and $\mathrm{Erfc}(u) = 1-\mathrm{Erf}(u) = \frac{2}{\sqrt{\pi}}\int_u^{\infty} e^{-t^2}dt$.

The asymptotic approximation that we have used for $K_0(\cdot)$ is accurate only for large values of the argument. Hence, accuracy of the integral in (20) depends on the value of βr_0. If we let $\beta r_0 \to 0$ we discover that while

$$\lim_{\beta r_0\to 0}\int_{\beta r_0}^{\infty} K_0(x)dx = \frac{\pi}{2},$$

$$\lim_{\beta r_0\to 0}\frac{\pi}{\sqrt{2}}\,\mathrm{Erfc}(\sqrt{\beta r_0}) = \frac{\pi}{\sqrt{2}}.$$

To improve the approximation in Eq. (20) for small values of βr_0, we introduce an additional factor as follows:

$$\int_{\beta r_0}^{\infty} K_0(x)dx \approx \frac{\pi}{2}\mathrm{Erfc}(\sqrt{\beta r_0})\frac{1/\sqrt{2}+10\beta r_0}{1+10\beta r_0}. \tag{21}$$

Defining:

$$Err_1 = \left|\int_{\beta r_0}^{\infty} K_0(x)dx - \frac{\pi}{2}\mathrm{Erfc}(\sqrt{\beta r_0})\right|,$$

$$Err_2 = \left|\int_{\beta r_0}^{\infty} K_0(x)dx - \frac{\pi}{2}\mathrm{Erfc}(\sqrt{\beta r_0})\frac{1/\sqrt{2}+10\beta r_0}{1+10\beta r_0}\right|,$$

numerical estimation shows that the additional factor improves the error of the approximation from $Err_1 < \pi/2 - \pi/\sqrt{2} = 0.65$ to $Err_2 < 0.067$.

Substituting Eq. (21) into Eq. (19), we finally have:

$$F(r_0) = \frac{1}{4\pi r_0^2}\left\{\frac{\gamma(1-\gamma)}{1-(1-\gamma)^2}(\sqrt{\beta\eta}r_0+1)e^{-\sqrt{\beta\eta}r_0}+\right.$$

$$\left.+\,\frac{2\gamma\eta r_0}{\pi}K_0(\beta r_0) + \frac{\sqrt{2}\gamma\eta}{\beta}\mathrm{Erfc}(\sqrt{\beta r_0})\frac{1/\sqrt{2}+10\beta r_0}{1+10\beta r_0}\right\}. \tag{22}$$

It is interesting to check two limiting cases. When there are no obstacles ($\eta = 0$), we have:

$$F(r_0) = \frac{1}{4\pi r_0^2}\left[\frac{\gamma(1-\gamma)}{1-(1-\gamma)^2} + \frac{\gamma}{1-(1-\gamma)^2}\right] = \frac{1}{4\pi r_0^2}$$

When there is no absorption ($\gamma = 0$), we have:

$$F(r_0) = \frac{1}{4\pi r_0^2}\left(\frac{1}{2} + \frac{1}{2}\right) = \frac{1}{4\pi r_0^2},$$

as in the case of propagation of a spherical wave in free space.

6 Relationships with the classical theory

The obvious starting point to characterize propagation in the wireless channel would be to use Maxwell equations. In principle, these can provide a complete characterization of the propagation loss in any given media. However, in the case of a rich scattering environment such as an urban area, this approach does not lead to closed form solutions. Hence, numerical solvers, empirical formulas, experimental measurements, and computer simulations are often used in practice.

Our approach, instead than looking for a complete solution for a given environment, consists in modelling a generic urban area as a random collection of scatterers, and in studying propagation in a random medium. We acknowledge the existence of a huge literature on propagation in random media which dates back to the beginning of last century, with the study of radiation of light in foggy atmospheres. Historically, the problem has been investigated from two distinct points of view. One is "radiative transfer theory" or "transport theory", and the other is "multiple scattering theory" or "analytical theory".

Radiative transfer theory is heuristic and deals directly with the transport of energy through a medium containing particles, it is based on the equation of radiative transfer, which is a differential equation equivalent to the Maxwell-Boltzmann collision equation used in the kinetic theory of gases and in neutron transport theory.

Analytical theory is more rigorous and starts with the wave equation or with Maxwell equations, obtains a solution for a single particle, introduces the interaction effects of many particles, and then considers statistical averages.

The two theories deal with the same phenomena, even though their starting points are different, therefore there are fundamental relationships between them. These are outlined in the classic book by Ishimaru [14], which shows (see chapter 14) that under certain approximations it is possible to derive the transport equation using analytical theory.

It is interesting that our proposed "wandering photon" model can also be related to transport theory, although it starts from different premises.

The (numerical) solution of the transport theory model in the case of a spherical wave radiating in a random medium of isotropic scatterers is outlined in chapter 12 of Ishimaru [14]. The transport equation reduces to an integral equation for the specific intensity (Eq. (12.4) in [14]) that is similar to our Eq. (12). However, the terms in the two equations have different meanings in the two models and are multiplied by different coefficients. Nevertheless, the functional form of the equation, and hence of the solution, is similar in the two cases. The similarity between Eq. (12.4) of Ishimaru and our Eq. (12) suggests that our *pdf* of the location where the random walk stops must be related to the specific intensity in transport theory. In the following we describe a power density model that explains this relationship.

6.1 Modelling the power density with random walks

We define the power density in our probabilistic model as the number of photons $N(r)$ per unit area that hit the external surface of a sphere of radius Δr centered at distance r from the source. We want to relate $N(r)$ to $G(r)$.

The number of photons absorbed inside the sphere of radius Δr is given by $G(r)(4\pi/3)\Delta r^3$. Letting l be the average path length of a photon inside the sphere, this quantity also equals the number of photons $N(r)4\pi\Delta r^2$ that enter the sphere times the absorption coefficient γ and the average number of reflections $\eta\ l$ experienced by a single photon inside the sphere. Clearly, $L = N(r)4\pi\Delta r^2\ l$ is the total path length of the photons inside the sphere, and we

have the equation:

$$\frac{4}{3}\pi\Delta r^3 G(r) = L\gamma\eta. \tag{23}$$

Similarly, in 2D we have $L = N(r)2\pi\Delta r\ l$, where $N(r)$ is the number of photons per unit length that enter a circle of radius Δr centered at distance r from the source, and Eq. (23) becomes:

$$\pi\Delta r^2 G(r) = L\gamma\eta. \tag{24}$$

A simple trigonometric exercise leads to the expression:

$$L = N(r)\frac{4}{3}\pi\Delta r^3$$

in 3D, and similarly in 2D:

$$L = N(r)\pi\Delta r^2.$$

Substituting the total path length L into Eqs. (23) and (24), we find the expression for the power density:

$$N(r) = \frac{G(r)}{\gamma\eta}. \tag{25}$$

6.2 Comparison with transport theory

We can now compare the analytical expressions of the power density and the power flux, derived within our model, with the corresponding transport theory quantities that can be derived numerically solving the equation of radiative transfer. A graphical comparison is depicted in Fig. 4, where our 3D formulas (22) and (25) are plotted on the right hand side of the figure, while similar plots, derived numerically in [14], appear on the left hand side. Note that to be coherent with Fig.12.3 of Ishimaru [14], we have normalized both plots by an r^2 factor.

There is no doubt that the graphical behavior of the two sets of curves is very similar. However, we can limit ourselves only to a qualitative comparison of the two plots, for two reasons. First, the parameters of the two theories are different: we use the absorption coefficient (γ) and the average step length ($1/\eta$) of the random walk, whereas transport

theory uses the particles number per unit volume (ρ) and the absorption, (σ_a) scattering (σ_s) and total, ($\sigma_t = \sigma_a + \sigma_s$) particles cross section. Second, the transport theory curves are parametrized by the albedo $W_0 = \sigma_s/\sigma_t$, that is not independent from the abscissa coordinate $\rho\sigma_t r$; whereas the wandering photon curves are parametrized by the absorption coefficient γ, that is totally independent from the abscissa coordinate ηr. Another difficulty is in the absence of an analytical solution for the transport theory approach, so that no direct comparison between equations is possible.

We note that on both plots, when we move towards a lossless medium ($W_0 \to 1, \gamma \to 0$), the flux (solid line) curves tend to the $1/r^2$ abscissa line; while the density (dashed line) curves tend to diverge, as they tend to $1/r$. This phenomenon of $1/r$ slow decay of the power density is known in transport theory and is due to part of the energy being reflected back towards the source. In general, when obstacles are mostly scattering, rather than absorbing, the power density plots reported in the figure can become greater than unity; on the contrary the total power flow in the radial direction, given by the power flux, can never be greater than the total source of power. A power density plot higher than one, corresponding to an attenuation rate slower than $1/r^2$, can be explained in our model by some of the photons being reflected back and re-visit the same location multiple times.

Table 1 sums up the behavior, according to our model, of the power flux and of the power density at large distance from the transmitter. We can provide an explanation of the decay laws depicted in the table in terms of the recurrence properties of random walks. Let us focus on the power density. According to our formulas, when obstacles are mostly scattering, the power density attenuates as $1/r$ in 3D and diverges, with a log singularity, in 2D. The explanation is that random walks in 2D are recurrent, hence, when there is no absorption, the same photon visits infinitely many times the same disc of radius ϵ. On the contrary, in 3D the probability of the random walk to re-visit the same sphere of radius ϵ is less than one, hence, perfectly reflecting scatterers lead only to a decrease of the rate of decay of the power density from $1/r^2$ to $1/r$, due to a finite number of recurrent visits and eventual diffusion of photons in space. Note that random walks recurrence properties do not effect the Power flux

decay law, because, according to its definition, the power flux simply measures the number of photons that are able to reach a given radial distance, hence does not count recurrent photons multiple times.

Part II: Experiments

7 Summary of Results

We apply the theoretical model presented in the first part of the paper to predict the path loss of a wireless channel. By using a non-linear regression algorithm we fit Eq. (22) and Eq. (25) to experimental data collected in a microcell located in an urban area and we measure the accuracy of the prediction by evaluating the root mean square error σ_{std} of the model on the measured data. The two equations that we use to fit experimental data correspond to two different ideal measurements: the power flux equation measures the flux of photons passing through an antenna of given area oriented toward the source; the power density equation measures the total number of photons passing through the antenna, coming from any direction. Hence, Eq. (22) is more suited to model directional receiving antennas, while Eq. (25) is more suited to model isotropic receiving antennas. However, we note that Eq. (25) counts photons multiple times, if they are reflected back towards the receiver. Our experimental analysis shows that in practice both formulas lead to a similar result of a propagation loss that, due to absorption, presents a smooth transition from free space propagation to exponential attenuation (see Fig. 2).

We summarize our experimental findings as follows:

- The propagation law predicted by our model is in good agreement with experimental data. To have an idea of the quality of the matching we perform monotonic regression [1], to find the best, in mean square, non-decreasing function fitting the data. This

function provides a lower bound on the minimum value of σ_{std} that can be achieved by any theoretical model of propagation. Comparing the σ_{std} obtained by fitting our model with the one achieved by monotonic regression, we find a less than $2dB$ increase.

- The values found for the parameters η and γ when fitting our model to the experimental data are very reasonable for their physical interpretation as density and absorption coefficient of the obstacles in the considered urban area, thus suggesting a possible direct use of our formulas without experimental tuning of the parameters. The parameters are are also very stable under random perturbation of the data.

- We introduce a simplified, exponential path loss formula that proves to be as powerful for prediction as the complete formulas derived in our model. The parameters of this simple formula, however, do not have any physical meaning and must be determined by fitting experimental data.

- We find that our model provides a superior fit to the data than the simple power law model (Hata formula [13]). In addition, it provides good theoretical ground to empirical models that use a transition from low to high order power laws to fit experimental data.

8 Data collection method

Experimental measurements, collected in Rome, Italy, are courtesy of Ericsson Telecomunicazioni SpA. The transmitting antenna was a vertical resonant dipole located at a height of 6m and transmitting a continuous wave (CW) at a frequency of 900MHz, with a radiated power $P_t = 6.3W$, transmitting gain $G_t = 2dB$, and $EIRP = P_t G_t = 40dBm$. The antenna was located in "Piazza dei Quiríti", in the "Prati" district of Rome, near the Vatican city, at 12.46591E latitute, 41.91017N longitude (see map in Fig. 5). The receiving antenna was mounted on top of a moving vehicle at a height of approximately 1.5m. The vehicle was equipped with a GPS, to record the position of each sampled data point, and drove around

the transmitting site (see right handside of Fig. 5). Each data point consisted of the received power averaged over 50 measurements along a path of 40 wavelengths (Lee method) .

Fig. 6 depicts the collected data: the received power is represented by a vertical line drawn at each data point. Fig. 7 depicts a view of the location where some of the measurements were taken and shows the presence of different scatterers in the environment. For subsequent analysis, a reduction in the size of the data was performed as follows. The receiving equipment rounded the smallest value of received power to -114dB; therefore, in order to have an un-biased set of data, we considered only points located at a radial distance from the transmitter less than 317m, for which the received power was always higher than -114dB. Moreover, the vehicle moving around the transmitting site collected a larger amount of data points as the radial distance from the transmitter increased. For example, a larger number of data points were collected on an ideal circle of radius 200m centered at the transmitting site, compared to the number of data points collected on an ideal circle of radius 50m. Hence, in order to remove this unwanted bias toward farther points, we averaged all data points inside annuli of 5m intervals, generating a uniform set of measurements along the radial direction. This corresponds to performing a local spatial average similar to the standard Lee method, but performed on a small annular area.

9 Model fitting

In order to fit the propagation loss formulas to the measured data we need to convert the densities in our 3D model expressed by Eqs. (22) and (25) to the actual received power of the antenna in our system. We do so by adding a multiplicative factor C to the formulas that takes into account for the transmitted power, gain of the transmitting antenna, effective area of the receiving antenna, and additional hardware losses in the system. Then we perform a non linear least squares procedure to determine values of C, η and γ that minimize the rms error σ_{std} from the sampled data.

By including the multiplicative factor C to Eqs. (22) and (25) we obtain an expression

for the power received by an antenna located at a distance r_0 from the transmitter of the type:

$$P_{recv}(r_0) = \frac{C}{r_0^2}\, f(\eta r_0, \gamma), \tag{26}$$

where $f(\cdot)$ is a function of the two dimensionless parameters ηr_0 and γ, and C is expressed in $[Wm^2]$ units. We use Eq. (26) to define the Path Loss at a given distance r_0 as the expression in dB:

$$PL(r_0) = -[P_{recv}(r_0)]_{dB}, \tag{27}$$

and the rms error of the predicted path loss from the sampled data as:

$$\sigma_{std} = \sqrt{\frac{\sum_{j=1}^{n}[PL_m(r_j) - PL(r_j)]^2}{n}},$$

where n is the number of measured data points, $PL_m(r_j)$ is the measured path loss at the jth point located at a radial distance r_j from the transmitter, and $PL(r_j)$ is the corresponding predicted path loss derived from Eq. (27). To minimize the rms error we use the standard MATLAB procedure `lsqnonlin()` that is a fairly sophisticated non linear least squares routine based on the Gauss-Newton algorithm. Accordingly (see Fig. 2), we find the values $\eta = 0.09$, $\gamma = 0.17$, $C = 0.065$, and a corresponding $\sigma_{std} = 3.72dB$, for the flux model; and the values $\eta = 0.12$, $\gamma = 0.12$, $C = 0.02$, $\sigma_{std} = 3.6dB$, for the power density model. These values correspond to having on average one obstacle every ten meters, with an absorption coefficient of $12\% \sim 17\%$. These values are very reasonable for the considered urban area and suggest that, in principle, values of the parameters that match the characteristics of the environment can be chosen without performing experiments, but by estimating directly the amount of clutter in the environment (i.e. the density of the scatterers), the absorption coefficient of the scatterers, and the gains and losses in the system. This method can be considerably less expensive than performing experiments, and can be used to obtain rough, initial guidelines on the path loss of a given environment.

9.1 Sensitivity of the model to noise

As indication of robustness of our theoretical model, we check if the physical parameters, absorption coefficient (γ) and average number of reflections per meter (η), are stable under random perturbation of the data. We do so by adding log-normal random noise of zero mean and standard deviation σ_{noise} to the data and determining, via non linear regression, the parameters η and γ for different values of σ_{noise}. Results are presented in Fig. 8. We note that the parameters are very stable under perturbations up to 7dB. This suggests that they capture real physical properties of the environment that are invariant to random noise. Moreover, we note that the values of the parameters predicted by the power flux model (continuous line) are very close to the values predicted by the power density model (dotted line), up to perturbations of 13dB; which implies that either of the two models models can be used to fit the parameters. For higher values of the perturbation noise, the flux model is more stable in predicting the everage number of reflections per meter η, while the density model is more stable in predicting the absorption coefficient γ.

9.2 A simplified exponential formula

For quick, practical calculation purposes, engineers may prefer to express the path loss using a simple formula, rather than the long formulas that we have derived in our model. The plots of these long formulas, depicted in Fig. 2, suggest a behavior that follows an inverse square law, with a smooth transition to an exponential law, as the distance between transmitter and receiver increases. Accordingly, we are led to the following simplified formula for path loss prediction:

$$PL^{-1}(r) = B\frac{e^{-br}}{r^2}. \tag{28}$$

The above formula proves to be as powerful in fitting the experimental data as the complete formulas derived directly from the theoretical model. In Fig. 9 we compare results of the simplified formula with the complete formula using the flux model. Values of the rms errors are practically indistinguishable at $\sigma_{std} = 3.72dB$ for the complete formula and $\sigma_{std} = 3.75dB$

for the simplified one. The physical meaning of the parameters is, however, lost in the simplified formula.

9.3 Comparison with Hata formula and best fit

Finally, we compare our results with the simple power law model (Hata formula [13]) and with the result of monotonic regression performed on the measured data. The monotonic regression [1] of a function is the best, in mean square, non-decreasing function fitting the data. It provides a lower bound on the minimum value of σ_{std} that can be achieved by any theoretical model of propagation: Any path loss prediction that does not depend on specific knowledge of an inhomogeneous environment, and in particular that is a function only of distance from the transmitter and general properties of the environment, must be a nondecreasing function of distance. The comparison is depicted in Fig. 10 and Table 2, and validates our model that closely follows the monotonic regression line depicted in Fig. 10.

In Fig. 10 it is also evident what is the typical problem of applying the simple Hata formula, popular in cellular systems design, to predict the path loss in microcellular systems: a power law with a fixed exponent (4.66 in this case) overestimates the real path loss in the close range, where the signal undergoes few reflections to reach the receiver and propagation is almost as in free space, and it underestimates the real path loss at larger distances, where there is an exponential attenuation, due to the absorption of many reflecting obstacles. Empirical formulas characterized by two different power laws, one with an exponent close to two, to be used close to the transmitter, and another with a high order exponent, to be used after a breakpoint distance, are better suited for prediction in this kind of environments and can be theoretically justified by our model.

10 Conclusion

We presented a new model of propagation for microcellular systems entirely based on probability theory, rather than on the classical theory of electromagnetics. We have solved the

model analytically and derived a power attenuation formula that can be applied to predict the path loss of a wireless channel. The main theoretical result is in predicting a path loss that follows (in 3D) an inverse square law with the distance to the transmitter, with a smooth transition to an exponential mode, as the distance between transmitter and receiver increases. This result gives theoretical ground to previously proposed empirical double exponent models that use a transition from low to high order power laws as the distance between transmitter and receiver increases. The model is based on two physical parameters that are used to model the propagation environment: the amount of clutter in the environment, and the absorption coefficient of the obstacles . We have validated our result through comparison with experimental data and we have introduced a simplified path loss formula that is as powerful for prediction as the complete formula derived theoretically, when its parameters are tuned by fitting experimental data.

We believe that the probabilistic approach exploited here is a powerful tool to describe the complex urban wireless channel. Future research directions include characterization of wide band channels and the study of second order moments, beside average quantities.

11 Acknowledgements

The authors would like to thank Ing. Sergio De Vita of Ericsson Telecomunicazioni SpA, for providing access to the experimental data reported in the paper.

References

[1] R. E. Barlow, D.J. Bartholomew, J.M. Bremner, and H.D. Brunk. "Statistical Inference under Order Restrictions: th Theory and Applications of Isotonic Regression." *John Wiley and Sons, 1972.*

[2] H. L. Bertoni, W. Honcharenko, L. Rocha Maciel, and H.H. Xia. "UHF Propagation Prediction for Wireless Personal Communications." *Proceedings of the IEEE, 82(9), pp. 1333-1359, 1994.*

[3] N. Blaunstein, R. Giladi, and M. Levin. "Characteristics' Prediction in Urban and Suburban Environments." *IEEE Transactions on Vehicular Technology, 47(1), pp. 225-234, 1998.*

[4] N. Blaunstein, and M. Levin. "Prediction of UHF-Wave Propagation in Suburban and Rural Environments." *Proceedings of the URSI Symposium on Communication, pp.191-200, 1995.*

[5] N. Blaunstein, and M. Levin. "VHF/UHF Wave Attenuation in a City with regularly distributed buildings." *Radio Science, 31, pp.313-323, 1996.*

[6] V. Erceg, L. Greenstein, S. Tjandra, S.R. Parkoff, A. Gupta, B. Kulic, A.A. Julius, and R. Bianchi. "An Empirically Based Path Loss Model for Wireless Channels in Suburban Environments." *IEEE Journal on Selected Areas of Communications, 17(7), pp. 1205-1211, 1999.*

[7] M.J. Feurstein, K. L. Blackard, T. Rappaport, S. Y. Seidel, H. H. Xia. "Path Loss, Delay Spread, and Outage Models as Functions of Antenna Height for Microcellular Systems Design." *IEEE Transactions on Vehicular Technology, 43(3), pp. 487-498, 1994.*

[8] G. Franceschetti, S. Marano, and F. Palmieri. "Propagation Without Wave Equation, Toward an Urban Area Model." *IEEE Transactions on Antennas and Propagation, 47(9), pp.1393-1404, 1999.*

[9] I.S. Gradshteyn and I.M. Ryzhik. *"Table of Integrals, Series, and Products." Fifth edition, A. Jeffrey Editor, Academic Press, 1994.*

[10] E. Green. "Path Loss and Signal Variability Analysis for Microcells." *Proceedings of the IEE fifth International Conference on Mobile and Personal Communications, pp.38-41, 1989.*

[11] L. Greenstein, N. Amitay, Ta-Shing Chu, L.J. Cimini Jr., G.J. Foschini, M.J. Gans, Chih-Lin I, A.J. Rustako Jr., R.A. Valenzuela, and G. Vannucci. "Microcells in Personal Communications Systems." *IEEE Communications Magazine, December, pp.76-88, 1992.*

[12] E. Grosswald. *"Bessel Polynomials." Lecture Notes in Mathematics 698. Springer Verlag, 1978.*

[13] M. Hata. "Empirical Formula for Propagation Loss in Land Mobile Radio Services." *IEEE Transactions on Vehicular Technology, 29(3), pp.317-325, 1980.*

[14] A. Ishimaru. "Wave Propagation and Scattering in Random Media." *Vol. 1,2, Academic Press, 1978.*

[15] L. Rocha Maciel, H. L. Bertoni, and H.H Xia. "Unified Approach to Prediction of Propagation Over Buildings for All Ranges of Base Station Antenna Height." *IEEE Transactions on Vehicular Technology, 42(1), 1993.*

[16] S. Marano, F. Palmieri, and G. Franceschetti. "Statistical characterization of ray propagation in a random lattice." *Journal of the Optical Society of America, 16(10), pp.2459-2464, 1999.*

[17] Y. Okumura, E. Ohmori, T. Kawano, and K. Fukuda. "Field Strength and its Variability in VHF and UHF Land-Mobile Radio Service." *Review of the Electrical Communication Laboratory, 16(9-10), pp. 825-873, 1968.*

[18] A.J. Rustako Jr, N. Amitay, G.J. Owens, and R.S. Roman. "Radio Propagation at microwave frequencies for Line of Sight Microcellular Mobile and Personal Communications." *IEEE Transactions on Vehicular Technology, 40, pp.203-210, 1991.*

[19] J.H. Tarng, and K.M. Ju. "A Novel 3-D Scattering Model of 1.8-GHz Radio Propagation in Microcellular Urban Environment." *IEEE Transactions on Electromagnetic Compatibility, 41(2), pp.100-106, 1999.*

[20] H.H. Xia, and H.L. Bertoni. "Diffraction of Cylindrical and Plane Waves by an Array of Absorbing Half-Screens." *IEEE Transactions on Antennas and Propagation, 40(2), pp. 170-177, 1992.*

[21] H.H. Xia, H.L. Bertoni, L. R. Maciel, A. Lindsay-Stewart, and R. Rowe. "Radio Propagation Characteristics for Line of Sight Microcellular and Personal Communications." *IEEE Transactions on Antennas and Propagation, 41(10), pp. 1439-1447, 1993.*

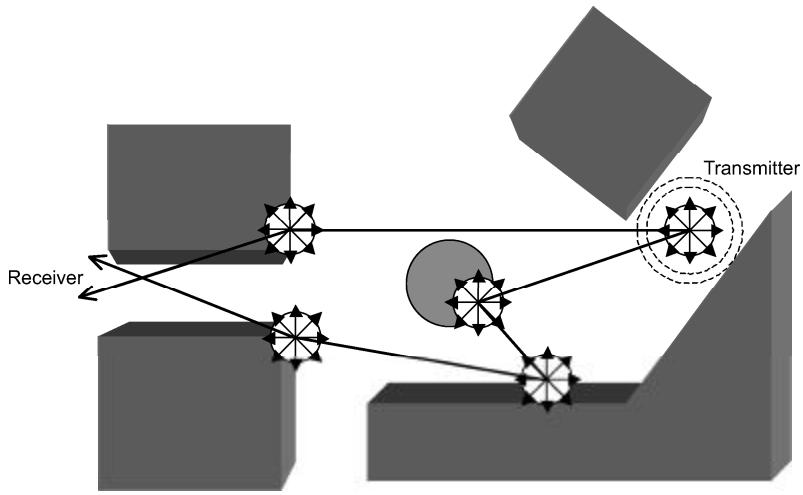

Figure 1: **Sketch of the propagation model.** *Each photon radiating from an isotropic source propagates in the environment following a piecewise linear trajectory, modelled as a random walk. Each time the photon hits an obstacle, it turns in a random direction, or it is absorbed by the obstacle.*

PARAMETERS	*OBSTACLES*	*Power Density, 2-D*	*Power Density, 3-D*
$\gamma \to 1$, $\eta > 0$	mostly absorbing	exponential attenuation	exponential attenuation
$\gamma \to 0$, $\eta r < \infty$	mostly scattering	∞	$\sim 1/r$
$\eta = 0$	no obstacles	$\sim 1/r$	$\sim 1/r^2$
		Power Flux, 2-D	*Power Flux, 3-D*
$\gamma \to 1$, $\eta > 0$	mostly absorbing	exponential attenuation	exponential attenuation
$\gamma \to 0$, $\eta r < \infty$	mostly scattering	$\sim 1/r$	$\sim 1/r^2$
$\eta = 0$	no obstacles	$\sim 1/r$	$\sim 1/r^2$

Table 1: **Power at large distance as predicted by our model.**

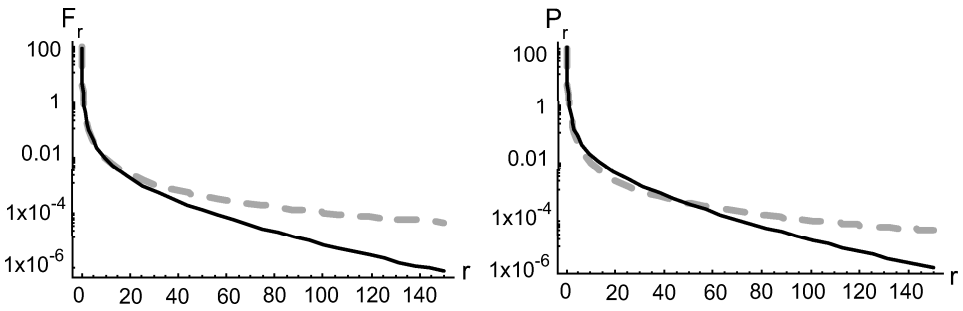

Figure 2: **Results of the model compared to free space propagation.** *The dashed line curves represent the free space $1/r^2$ attenuation law, the continuous line curves represent the predicted power flux F_r (left handside of the figure) and power density P_r (right handside of the figure) of our 3D probabilistic model. We note that the flux model presents a smooth transition from the $1/r^2$ law to an exponential attenuation; the power density model, although providing a very similar fit, predicts slightly higher power near the source. The breakpoint at which the model starts diverging from the $1/r^2$ law ($r \approx 30m$ in the figure) is determined by the values of η and γ. In the figure these values are determined from the experiments presented in part II of this paper.*

Model	σ_{std}	*Exponent*	*Multiplicative Factor*
$PL^{-1}(r) = A(\frac{1}{r})^a$	$6.053dB$	$a = 4.66$	$A = .0034$
$PL^{-1}(r) = B\frac{e^{-br}}{r^2}$	$3.75dB$	$b = 0.028$	$B = .0765$
Monotonic Regression	$2.04dB$		

Table 2: **Regression Results.** *The first line of the Table is relative to the Hata formula. The second line is relative to the simplified formula of eq. (28). The third line is relative to monotonic regression.*

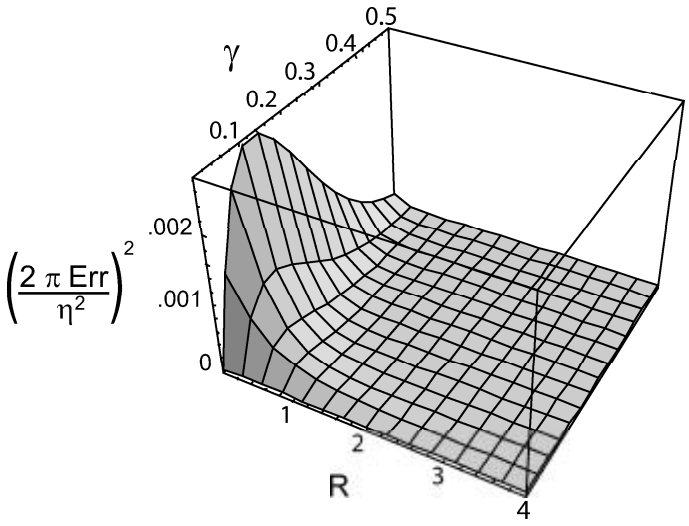

Figure 3: **Estimate of the Error.** *The plot depicts an estimate of the squared error of the approximation.*

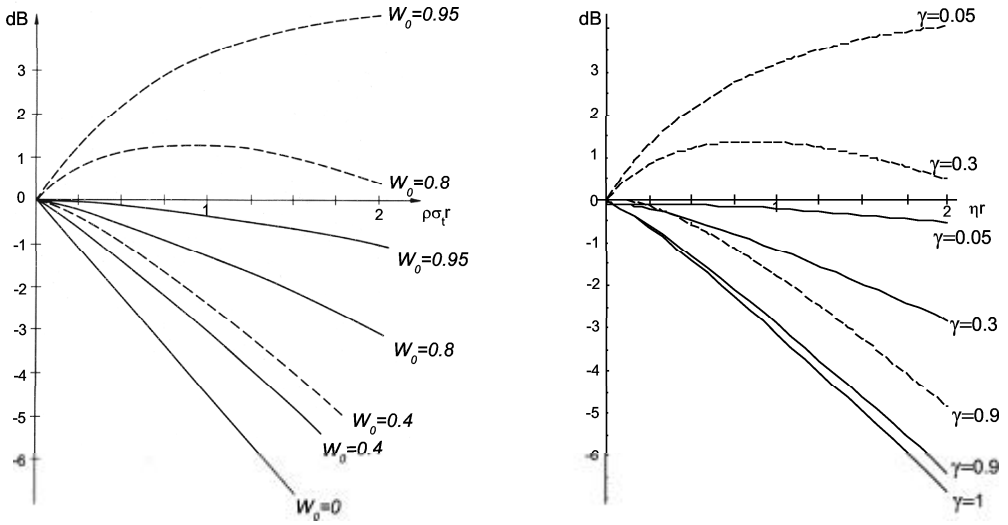

Figure 4: **Power Flux and Power Density.** *The dashed curves represent the power density (normalized by an r^2 factor), and the solid line curves represent the power flux (normalized by an r^2 factor). Left hand side: results from transport theory obtained numerically solving the equation of transfer. Right hand side: analytical results according to the wandering photon model.*

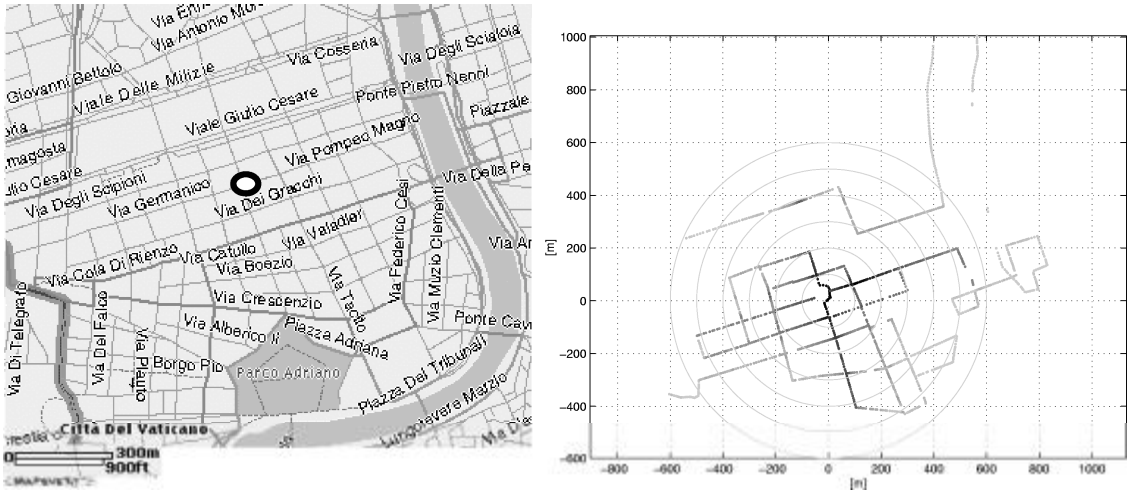

Figure 5: **Measurements location.** *Measurements were taken in the "Prati" district of Rome, near the Vatican city. The transmitting antenna was placed in "Piazza dei Quiríti", which is highlighted by the black circle in the map on the left handside of the figure. The right hand side of the figure shows the path taken by the van as it drove around the transmitting site. Each data point is shown with a grey level proportional to the power of the received signal. Circles centered at the transmitting site are drawn with increasing radii of* $100m$ *steps. The map on the left hand side of the figure is taken from* `http://www.mapquest.com` *. Power level measurements are courtesy of Ericsson Telecomunicazioni SpA.*

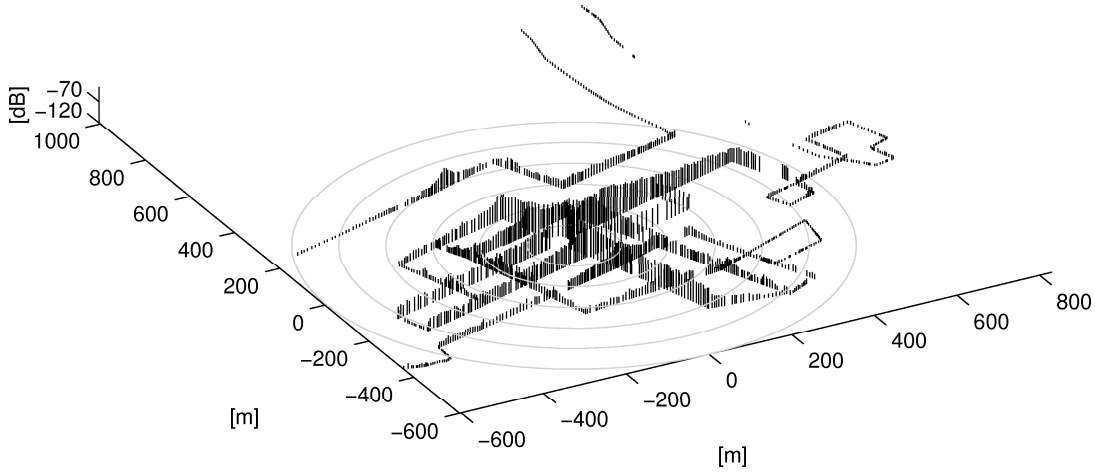

Figure 6: **Plot of the received power.** *A vertical line is drawn at each data point. The height of the line corresponds to the value of the received power expressed in dB. Circles centered at the transmitting site are drawn with increasing radii of* $100m$ *steps.*

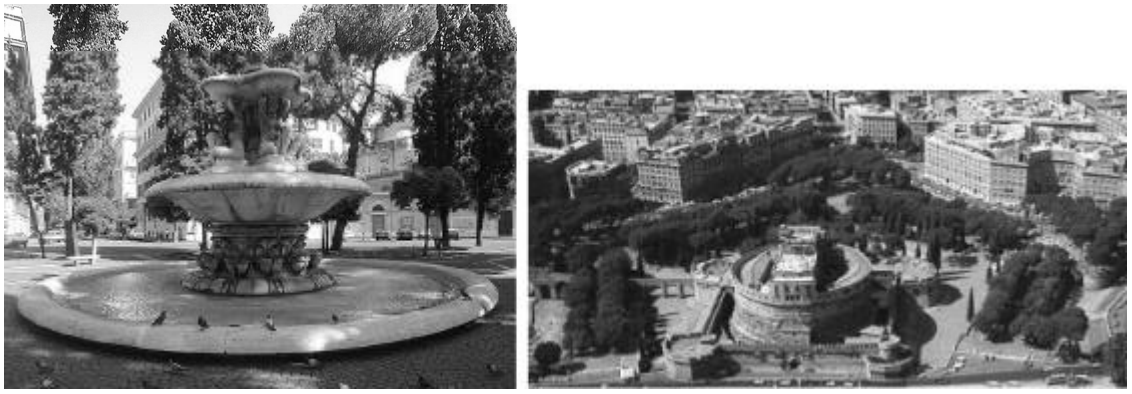

Figure 7: **View of the location.** *The left handside of the figure depicts "piazza dei Quiríti", where the transmitting antenna was located. The right handside of the picture depicts a view of "Parco Adriano" and of the surrounding streets where some of the measurements were taken.*

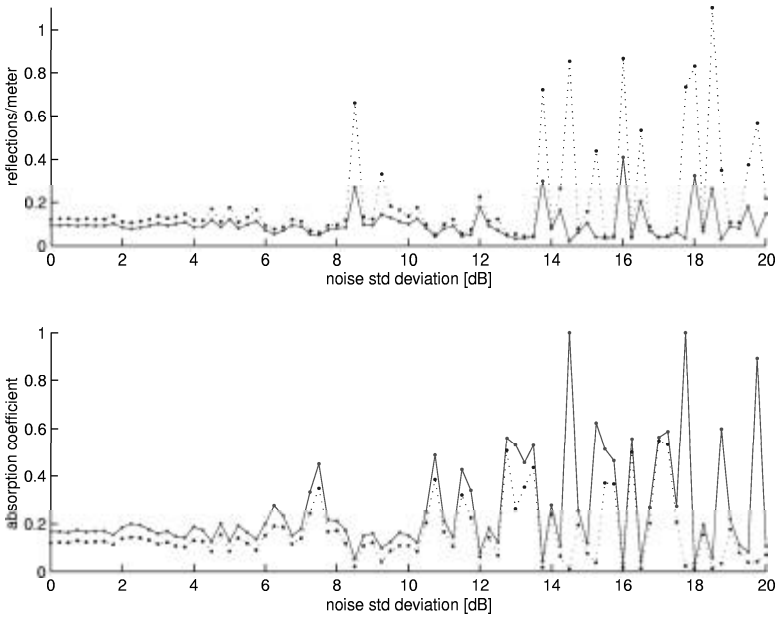

Figure 8: **Sensitivity analysis.** *Predictions of the flux model are indicated with continuous lines, predictions of the density model are indicated with dotted lines.*

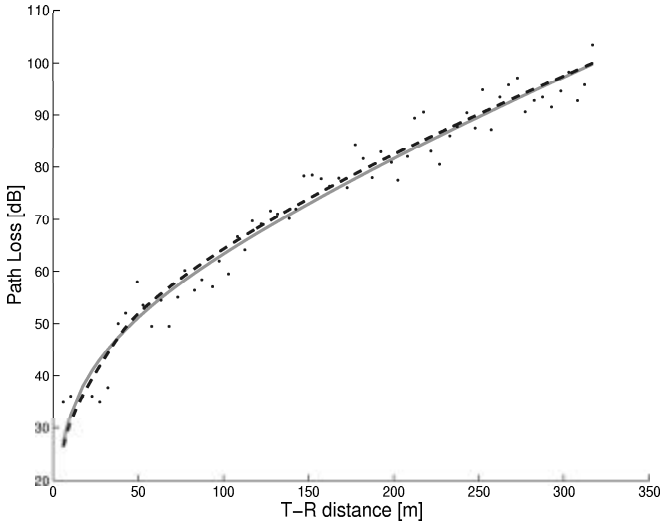

Figure 9: **Complete vs. simplified formula.** *The scattered points represent measured data. The dashed line represent the fit of the data using our flux model. The continuous line represents the fit of the data using our simplified formula (28). The rms error of the flux model, is* $\sigma_{std} = 3.72dB$*; the rms error of the simplified formula is* $\sigma_{std} = 3.75dB$*.*

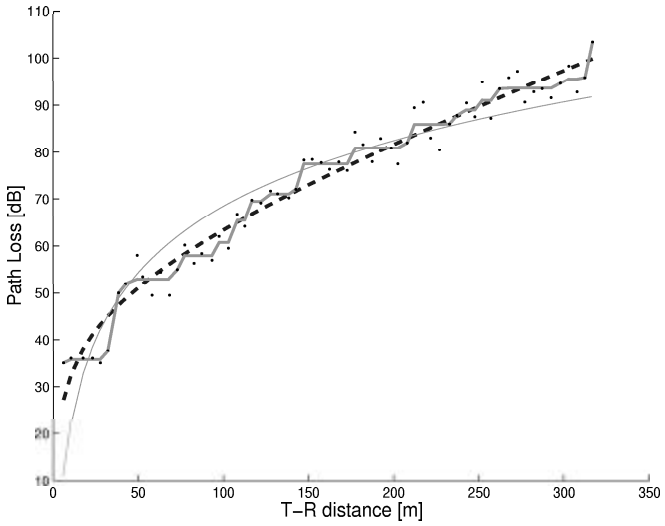

Figure 10: **Comparison.** *The dashed line represent the fit of the data using the simplified path loss formula. The thin continuous line represents the fit of the data using a power law. The "staircase" line is the result of the monotonic regression, representing the best non-decreasing function fitting the data. Values of the rms error are reported in Table 2.*